Bandgap structure of thermally excited surface phonon polaritons

Igal Balin, Nir Dahan, Vladimir Kleiner, and Erez Hasman

Citation: Appl. Phys. Lett. **96**, 071911 (2010); doi: 10.1063/1.3319539
View online: http://dx.doi.org/10.1063/1.3319539
View Table of Contents: http://aip.scitation.org/toc/apl/96/7
Published by the American Institute of Physics

Bandgap structure of thermally excited surface phonon polaritons

Igal Balin, Nir Dahan, Vladimir Kleiner, and Erez Hasman[a)]
Micro and Nanooptics Laboratory, Faculty of Mechanical Engineering and Russell Berrie Nanotechnology Institute, Technion–Israel Institute of Technology, Haifa 32000, Israel

(Received 29 December 2009; accepted 24 January 2010; published online 18 February 2010)

A wide bandgap of thermally excited surface phonon polaritons (SPhPs) is experimentally observed. Formation of the bandgap and coupling to radiative waves is done by a binary biharmonic structure formed on a SiC substrate. The bandgap width is controlled by the ratio of the two harmonic magnitudes of the structure's profile. The characteristic one-dimensional Van Hove singularity is experimentally observed in the spectral density of states of the SPhPs. Moreover, an inverse relation is found between the gap width and the squared spatial coherence length of the emitted thermal radiation, as predicted by theoretical calculations. © *2010 American Institute of Physics*. [doi:10.1063/1.3319539]

Conventional thermal sources usually have a broad spectrum and isotropic emittance. However, recent works have shown that coherent thermal emission can be obtained by electromagnetic surface waves excitation.[1–4] Surface waves are confined waves due to collective oscillations of the free electrons in metals (surface plasmon polaritons, SPPs) or resonant collective vibrations in polar materials (surface phonon polaritons, SPhPs). The emission properties, such as coherence length or energy density, can be engineered by modifying the dynamics of the surface waves, for instance, by localization.[5,6] One of the ways to achieve this localization is by introducing a Bragg grating on the surface of the polaritonic material which results in a bandgap in the dispersion curve.[7] At the bandgap's edges, the density of the surface modes has a Van Hove singularity,[8] thus the field is strongly enhanced near the air-substrate interface. This can be exploited to enhance second harmonic generation,[9] Raman scattering,[10] photoluminescence,[11] fluorescence,[12] and absorption. A convenient method of observing these energy gaps is by coupling the polaritons to propagating waves. For this purpose, an additional grating component is essential.[7] By composing the Bragg and the coupler components a biharmonic structure is created such that the radiative waves carry information about the bandgap. In many cases, a large gap width is required. For example, when introducing a defect inside the Bragg grating, localization of modes with frequencies inside the bandgap is allowed.[13,14] As the gap width increases, the localized modes are resolved more clearly. It was shown that the plasmonic gap width depends on the real part of the complex permittivity of metal, $\delta\omega \propto 1/\sqrt{|\varepsilon'|}$.[7] Since surface waves are excited in the spectral region where $\varepsilon'(\omega) < -1$, the largest gap width is expected to be found near the resonance frequency, corresponding to $\varepsilon'(\omega) \sim -1$. According to Wien's law, thermal emission has its maximum value in the mid-infrared (mid-IR) region at room temperature. Since the resonance frequency in metals is usually located in the ultraviolet/visible spectra range, only a small bandgap was observed in the mid-IR region.[15] In order to achieve a wide bandgap, it is reasonable to use polar materials such as SiC or SiO_2 which have resonance frequencies in the mid-IR region.

In this letter, we experimentally observe a wide bandgap of thermally excited SPhPs. Formation of the bandgap and coupling to the radiative waves is produced by a biharmonic structure formed on a SiC–6H substrate. The biharmonic function is quantized to two discrete levels, which we will refer to, hereafter, as a binary biharmonic structure (BBS). The energy gap width monotonically increases as a function of the relative amplitude of the Bragg harmonic. We experimentally verified that the density of states (DOS) near the bandgap has a characteristic one-dimensional (1D) Van Hove singularity. In addition, an inverse relation was found between the gap width and the squared spatial coherence length of the emitted thermal radiation at the band extrema frequencies, whereas the spectral quality factor remained constant. This feature can be utilized to design thermal emitters, polaritonic bandgap microcavities for sensing applications, and thermophotovoltaic systems.

SPhPs are excited on SiC in the mid-IR region, for which the real part of the complex permittivity is smaller than -1 (10.6–12.5 μm wavelength). The dispersion relation of SPhPs on a smooth surface is given by $k_{\mathrm{SPhP}} = k_0\sqrt{\varepsilon_s\varepsilon_a/(\varepsilon_s+\varepsilon_a)}$, where k_0 is the wave number of the electromagnetic wave in a vacuum, and ε_s and ε_a are the substrate and superstrate complex permittivites, respectively; in our case $\varepsilon_a = 1$ for air. The dispersion relation behavior is modified by introducing a periodic corrugation on the surface. If the wave vector of the corrugation is $2k_{\mathrm{SPhP}}$, then Bragg scattering of the surface wave occurs. Two standing wave solutions with different energies and the same wave number are obtained: thus, a bandgap appears in the dispersion curve.[16] In order to couple the SPhPs to propagating waves, an additional grating component with a wave number k_{SPhP} needs to be introduced. To fulfill these two functions, such a structure should have a profile that can be described as the sum of two harmonic components: $S(x) = A_1 \sin(Kx) + A_2 \sin(2Kx+\phi)$, where x is the spatial coordinate, $K = 2\pi/\Lambda$ is a grating wave number, Λ is the grating period, and ϕ is a relative phase between the Bragg and the coupler harmonics, see Fig. 1(a). We formed the BBS by operating the Heaviside step function $U[\ ]$ on the profile with $\phi = 0$, $s(x) = U[S(x)] = a_0/2 + \Sigma_{m=1}^{\infty} a_m \sin(mKx + \varphi_m)$. Figure 1(c) shows a typical power spectrum of the biharmonic structure with a Bragg to coupler harmonics ratio $A_2/A_1 = 4/5$. Figure

a)Electronic mail: mehasman@tx.technion.ac.il.

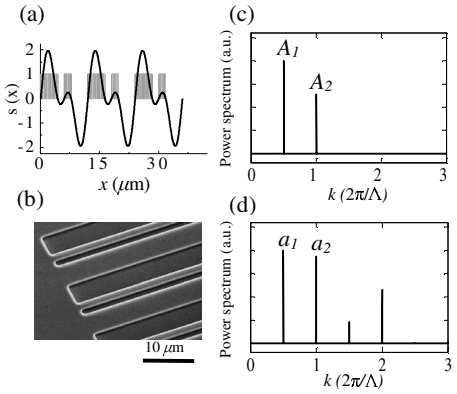

FIG. 1. (a) Schematic representation of a BBS obtained by binarization of a biharmonic structure with a Bragg to coupler harmonics amplitude ratio $A_2/A_1=4/5$ and $\phi=0$. (b) SEM image of realized BBS with period $\Lambda=11.2$ μm, depth $h=510$ nm, and $A_2/A_1=1$. (c) Power spectrum of biharmonic structure shown in Fig. 1(a). (d) Power spectrum of BBS shown in Fig. 1(a); (zero order is not shown).

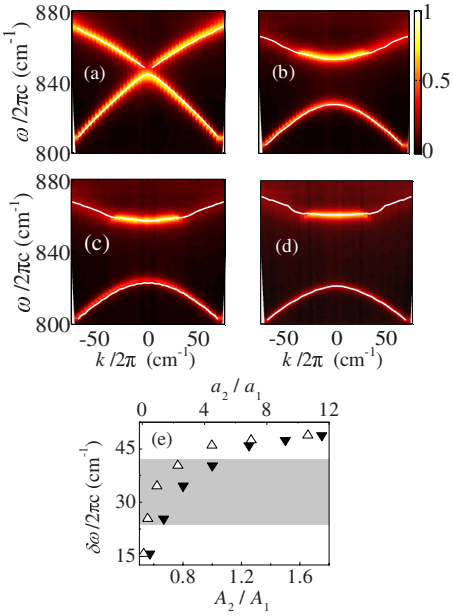

FIG. 2. (Color online) Measured dispersion of thermal emission from (a) binary coupler grating, and BBSs with (b) $A_2/A_1=2/3$, (c) $A_2/A_1=4/5$, and (d) $A_2/A_1=1$. RCWA calculations are depicted by solid white lines. (e) Calculated bandgap width of BBSs as a function of A_2/A_1 (solid, down triangles), and as a function of the ratio of the first two harmonics in the power spectrum a_2/a_1 (open, up triangles). The gray rectangle covers the points that were experimentally investigated.

1(d) shows the power spectrum of BBS with the same ratio of A_2/A_1. As can be seen, the two dominant harmonics of the BBS are the same as that of the biharmonic structure. Therefore, while we expect both structures to demonstrate similar behavior, the binarization method has a significant advantage in fabrication since a single mask is sufficient.

We investigate theoretically and experimentally thermal emission from a binary coupler grating ($U[S(x)]$ for which $A_2=0$) and BBSs with various amplitude ratios of A_2/A_1. The samples were fabricated using standard photolithographic techniques on a SiC substrate,[2] with a periodicity $\Lambda=11.2$ μm, depth $h=510$ nm, and filling factor 0.5. A scanning electron microscope (SEM) image of the magnified area is shown in Fig. 1(b). The selected periodicity of the structures ensured coupling of the surface waves at the resonance frequency $\omega_0/2\pi c=844$ cm^{-1} (corresponds to $\lambda_0=11.84$ μm) to radiative waves at a normal direction, according to the momentum matching condition $k_0 \sin\theta = k_{\mathrm{SPhP}}+qK$, where θ denotes the emission angle and q is the diffraction order. Measurements were performed using a Fourier transform IR spectrometer (Bruker, Vertex 70) while heating the sample to 773 K. Figure 2(a) shows the dispersion of SPhPs measured by thermal emission from the binary coupler grating normalized by the emission of a blackbody at the same temperature, along with a theoretical calculation based on a rigorous coupled-wave analysis (RCWA) method. The bright colors represent high emissivity. Although the binary coupler grating substantially consists the coupler harmonics, a small bandgap (normalized gap width $\delta\omega/\omega_0=3\cdot10^{-3}$) appears in the central region. Herein, it is clear that the Bragg harmonics originate from the binarization process of the profile. Moreover, the coupling strength of the upper branch is reduced to zero. This signature finding was studied in plasmonic bandgap structures: a grating that excites SPPs and has a profile distorted from a pure sinusoidal form,[7,11] and a binary coupler grating.[15] The bandgap width is proportional to the grating depth,[7,15] so that in a shallow grating ($h=300$ nm), a bandgap does not appear.[2] The measured and the calculated emissions from the BBSs are shown in Figs. 2(b)–2(d). Wide bandgaps are observed: $\delta\omega/\omega_0=0.03$, 0.04, and 0.05 for $A_2/A_1=2/3$, 4/5, and 1, respectively. These large gaps could be attributable in the mid-IR to the small permittivity of SiC in this spectrum. For comparison, we calculated the normalized gap width in a BBS on gold with $A_2/A_1=2/3$, $\Lambda=11.6$ μm, and $h=300$ nm; this yielded a tiny gap $\delta\omega/\omega_0=5.7\cdot10^{-3}$ at the same ω_0 as the BBS on SiC. The gap width dependence on the ratio of the amplitude of the Bragg harmonics normalized by the amplitude of the coupler A_2/A_1 and a_2/a_1 in the BBS is summarized in Fig. 2(e). As can be seen, the gap width increases as the ratio between the first two harmonics increases.

The spectral emissivity, derived from the cross sections of Figs. 2(a)–2(d) at $k=0$ (normal observation angle) is shown in Fig. 3(a). The spectral quality factor is found to be approximately constant among the BBSs, $Q=\omega_0/\Delta\omega\approx180$ where $\Delta\omega$ is the spectral peak width at half maximum. A typical angular distribution is shown in Fig. 3(b) for air (upper) and dielectric (lower) band edge frequencies (at $A_2/A_1=2/3$). The spatial coherence length in the vicinity of the bandgap can be derived as follows: using Taylor expansion near the bandgap, we represent the dispersion relation as $\Delta\omega\approx(1/2)d^2\omega/dk^2(\Delta k)^2$. The gap width $\delta\omega$ depends on the dispersion curvature $1/\delta\omega\propto d^2\omega/dk^2$, which is analogous to nondegenerate $k\cdot p$ perturbation theory in solid-state physics, where the effective mass is proportional to the gap width.[17] In addition, the angular lobe width is inversely proportional to the coherence length as $\Delta k\approx2\pi/l_c$. Therefore, the spatial coherence length depends on the temporal coherence and the gap width, $l_c\propto(\Delta\omega\delta\omega)^{-1/2}$. Figure 3(c) shows the coherence length at the extrema of the dielectric band as a function of gap width. Herein, the spectral quality factor is constant demonstrating that there is a trade-off between the coherence length and the gap width, $l_c\propto1/\sqrt{\delta\omega}$. According to Kirchhoff's law, enhanced emission of a BBS corresponds to enhanced absorption. Thus, a narrow absorption spectral resonance can be obtained in a wide range of angles utilizing a wide bandgap structure. This property can be exploited to

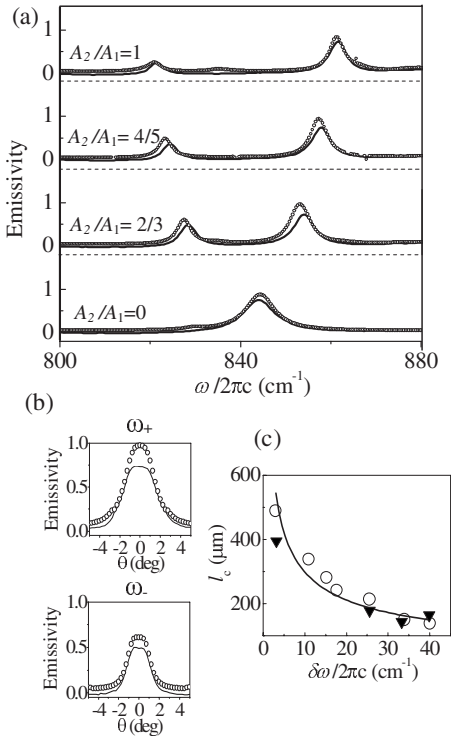

FIG. 3. Cross sections taken from Figs. 2(a)–2(d). (a) Spectral emissivity of BBSs vs frequency in a normal direction (k=0). (b) Angular emissivity of BBS with A_2/A_1=2/3 at air (upper) band and dielectric (lower) band extrema of the bandgap; experimental results (solid lines) and RCWA calculations (open circles). (c) Spatial coherence length of thermal emission of BBSs at dielectric band edge as a function of bandgap width; experimental results (solid, down triangles), RCWA calculations (open circles), and inverse square root fitting function (solid line, see text for details).

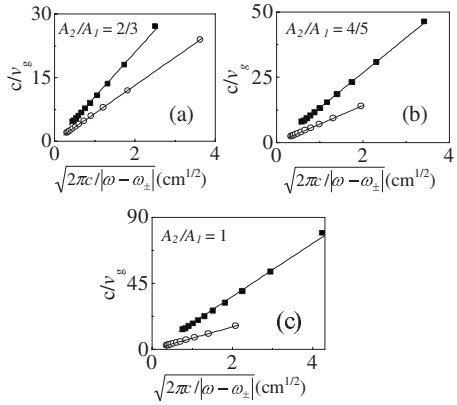

FIG. 4. Inverse group velocity of SPhPs normalized to speed of light in vacuum vs $1/\sqrt{|\omega-\omega_\pm|}$ ($\omega_\pm$ is the air band and dielectric band extema, respectively) obtained from the experimentally dispersion relations of BBSs with (a) A_2/A_1=2/3, (b) A_2/A_1=4/5, and (c) A_2/A_1=1. Solid squares denote air band; open circles denote dielectric band. Solid lines indicate linear curve fit with intersection at $|\omega-\omega_\pm|$=0.

design a mid-IR refractive-index sensor based on spectral resonant excitation of SPhPs,[18] which will not require a high coherence thermal source.

To further investigate the bandgap behavior, we evaluate the DOS of the SPhPs from their dispersion curves as follows: $\mathrm{DOS}(\omega)=\int dk\,\delta(\omega-\omega(k))\propto|d\omega/dk|^{-1}=1/v_g$, where v_g is the group velocity. In periodic structures, the group velocity vanishes at the bandgap edges. At these frequencies, there is a Van Hove singularity of the DOS with a characteristic behavior related to the structure's dimension.[8] In the 1D case, the DOS diverges as $[\pm(\omega-\omega_\pm)]^{-1/2}$, where $\omega_\pm$ is the air band and dielectric band edge frequencies, respectively. We calculated the group velocity from our measurements [Figs. 2(b)–2(d)] near the bandgap edge frequencies and observed that in BBSs, the DOS linearly depends on $[\pm(\omega-\omega_\pm)]^{-1/2}$, as expected from the Van Hove theorem. These results are shown in Figs. 4(a)–4(c) for all the fabricated structures, with a good agreement for both air band and dielectric band. As can be seen, the DOS in the air band is higher than in the dielectric band. According to Fermi's golden rule, the coupling strength between the surface waves and the radiative waves is proportional to the DOS of SPhPs. Consequently, higher emissivity in the air band is experimentally observed, as can be seen in Fig. 3(a).

To conclude, we investigated the bandgap of SPhPs by thermal emission from BBSs. At the band extrema, the spatial coherence length is determined by the gap width. Opening a large bandgap modifies the dynamics of the delocalized surface waves which can be exploited to enable the design of unconventional thermal sources, and the creation of a localized mode inside the bandgap according to the structure morphology and material properties. Moreover, the slow modes which result in a high DOS near the bandgap can be utilized for biosensing and detection applications in the mid-IR region.

This research was supported by the Israel Science Foundation and Russell Berrie Nanotechnology Institute.

[1] J.-J. Greffet, R. Carminati, K. Joulain, J.-P. Mulet, S. Mainguy, and Y. Chen, Nature (London) **416**, 61 (2002).
[2] N. Dahan, A. Niv, G. Biener, Y. Gorodetski, V. Kleiner, and E. Hasman, Phys. Rev. B **76**, 045427 (2007); J. Heat Transfer **130**, 112401 (2008).
[3] K. Ikeda, H. T. Miyazaki, T. Kasaya, K. Yamamoto, Y. Inoue, K. Fujimura, T. Kanakugi, M. Okada, K. Hatade, and S. Kitagawa, Appl. Phys. Lett. **92**, 021117 (2008).
[4] N. Dahan, A. Niv, G. Biener, V. Kleiner, and E. Hasman, Appl. Phys. Lett. **86**, 191102 (2005).
[5] J. A. Schuller, T. Taubner, and M. L. Brongersma, Nat. Photonics **3**, 658 (2009).
[6] L. J. Klein, S. Ingvarsson, and H. F. Hamann, Opt. Express **17**, 17963 (2009).
[7] W. L. Barnes, T. W. Preist, S. C. Kitson, and J. R. Sambles, Phys. Rev. B **54**, 6227 (1996).
[8] L. Van Hove, Phys. Rev. **89**, 1189 (1953).
[9] A. C. R. Pipino, R. P. Van Duyne, and G. C. Schatz, Phys. Rev. B **53**, 4162 (1996).
[10] A. Kocabas, G. Ertas, S. Seckin Senlik, and A. Aydinli, Opt. Express **16**, 12469 (2008).
[11] S. C. Kitson, W. L. Barnes, and J. R. Sambles, Phys. Rev. B **52**, 11441 (1995).
[12] Y. Wang and Z. Zhou, Appl. Phys. Lett. **89**, 253122 (2006).
[13] J.-C. Weeber, A. Bouhelier, G. Colas des Francs, L. Markey, and A. Dereux, Nano Lett. **7**, 1352 (2007).
[14] E. Descrovi, V. Paeder, L. Vaccaro, and H.-P. Herzig, Opt. Express **13**, 7017 (2005).
[15] G. Biener, A. Niv, V. Kleiner, and E. Hasman, Appl. Phys. Lett. **92**, 081913 (2008).
[16] E. Yablonovitch, Phys. Rev. Lett. **58**, 2059 (1987).
[17] J. Bardeen, J. Chem. Phys. **6**, 367 (1938).
[18] I. Balin, N. Dahan, V. Kleiner, and E. Hasman, Appl. Phys. Lett. **94**, 111112 (2009).